IEEE Access
Multidisciplinary ⋮ Rapid Review ⋮ Open Access Journal

Received 6 February 2024, accepted 28 February 2024, date of publication 1 March 2024, date of current version 7 March 2024.

Digital Object Identifier 10.1109/ACCESS.2024.3372411

RESEARCH ARTICLE

Miniaturization and Fabrication of a Novel Cross-Fractal Biosensor and Sensor for Characterizing 3D Printing Electromagnetic Properties in Polylactic Acid

MEZACHE ZINELABIDDINE[1], ABDULLAH ALZAHRANI[2], ABDULLAH ALWABLI[3], AMAR JAFFAR[4], ENAS ALI[5,6], AND MOHAMMED S. ALZAIDI[2]

[1]Institute of Optics and Precision Mechanics, University of Ferhat Abbas Setif, Setif 19000, Algeria
[2]Department of Electrical Engineering, College of Engineering, Taif University, Taif 21944, Saudi Arabia
[3]Department of Electrical Engineering, College of Engineering and Computing in Al-Qunfudhah, Umm Al-Qura University, Mecca 24382, Saudi Arabia
[4]Computer and Network Engineering Department, College of Computing, Umm Al-Qura University, Mecca 21955, Saudi Arabia
[5]Faculty of Engineering and Technology, Future University in Egypt, New Cairo 11835, Egypt
[6]Centre of Research Impact and Outcome, Chitkara University Institute of Engineering and Technology, Chitkara University, Rajpura, Punjab 140401, India

Corresponding authors: Enas Ali (enas.ali@fue.edu.eg) and Mezache Zinelabiddine (zinemezaache@yahoo.fr)

This work was supported by the Deanship of Graduate Studies and Scientific Research, Taif University.

ABSTRACT This study presents a new approach for characterizing the 3D printing electromagnetic properties in Polylactic Acid (PLA) using a novel cross-fractal sensor. The CST Studio Suite simulation, employing the finite element method (FEM), and the ADS simulation software, based on the equivalent circuit of this novel sensor, are utilized to enhance confidence in the convergence of simulation and measurement results. The analysis confirms that the real sensor, based on a cross-sectional fractal resonator, exhibits excellent sensitivity, selectivity, and linearity. Sensor performance is evaluated through two methods: the frequency-based approach and the S11 parameter analysis. In the frequency-based method, the sensor demonstrates a typical sensitivity of 0.0302 GHz/cm^3, while in the S11 parameter analysis, it exhibits a typical sensitivity of 0.3065 dB/cm^3. These results underscore the high sensitivity and linearity of this innovative sensor. The using of this novel cross fractal sensor, it promises to show how to properly adjust 3D printer parameters, potentially setting the ''infill percentage'' of the 3D print, this is because the proportion of air present changes when the printing percentage is changed, which can lead to (εr) and loss-tangent (tan (δ)) with varying the infill percentage, by the resonance frequency (fr) approach demonstrates a characteristic sensitivity of 0.1822 GHz/RIU. The experimental study confirmed that the fabricated sensor exhibits miniaturization (with an electrical size of λ0/8), high sensitivity, and excellent linearity in the frequency approach, with a typical sensitivity of 0.004615 GHz/%. The suggested biosensor demonstrated its capability to detect low concentrations of ethanol. These aqueous solutions, containing known alcohols like ethanol in low concentrations, enables identification of Halal and alcohol-free products in food sensing applications.

INDEX TERMS Fractal forms, 3D printing, sensor, biosensor, network analyzer, loss-tangent, sensitivity, permittivity.

I. INTRODUCTION

In 1988, Dr. Nathon Conen successfully developed the first fractal resonator that met various user requirements, such as compact size, wider bandwidth, affordable price and ease of fabrication. The term ''fractal'' was originally introduced by B. Mandelbrot, derived from the Latin word ''fractus'', which means irregular or broken. Resonator technology requires the creation of antennas with wider bandwidths and smaller sizes than traditional resonators to improve communication

The associate editor coordinating the review of this manuscript and approving it for publication was Norbert Herencsar.

systems. Famous mathematicians such as W. Sierpinsky, N. Von Koch, D. Hilbert and H. Minkowski have significantly contributed to fractal geometry [1]. Their fractal concepts inspired the resonator engineering community to explore the potential use of these geometries in antenna research and design in Ghz regime to minimize the size of the antennas which has a high radiation efficiency, they are considered the fractal geometry in the manufacturing of the antennas [2], [3], [4]. In references [5], [6], [7], [8], [9], and [10], fractal forms were utilized to enhance antenna characteristics, whereas a combination of metamaterials and fractal shapes was employed to improve properties in references [11], [12], [13], and [14]. Using fractal forms at the nanotechnology level has proven its importance in improving the antenna characteristics in the Terahertz Regime [15]. Recent works have also demonstrated the importance of using fractal shapes in the biosensor field to improve its properties in identifying viruses and diseases, such as diabetes and cancer [16], [17], [18], [19].

Recent research has concentrated on the use of fractal sensor for knowing 3D printing properties in Polylactic Acid (PLA), yielding promising results. One notable advantage of employing fractal resonators is their ability to detect a broad spectrum of frequencies, thus facilitating the recognition of 3D printing properties across different frequency ranges. Furthermore, fractal resonators exhibit heightened resistance to noise and interference, enabling them to maintain accuracy in recognizing 3D printing properties [20]. The proposed cross-sectional fractal resonator sensor controls the different properties of fractal geometry to improve the recognition of 3D printing objects in Polylactic Acid (PLA). Fractals exhibit self-similarity across various scales, enhancing sensitivity and pattern recognition accuracy. This novel resonator design into the detection system significantly improves the accuracy and reliability of recognizing 3D printing electromagnetic properties. The application of this groundbreaking fractal cross-resonator extends to the field of artificial intelligence, especially in the development of intelligent systems capable of recognizing and understanding 3D printing properties. This sensor can be utilized in smart sensor networks and radio-frequency identification (RFID) systems. Its compact size and multiband capabilities make it suitable for integration into small sensors, tags, and devices used in intelligent systems.

The scientists assessed the performance of the resonator for recognizing 3D printing properties in Polylactic Acid (PLA) [20]. The resonator consistently demonstrated accurate recognition of 3D printing properties in Polylactic Acid (PLA), even in the presence of noise and interference [20]. The researchers conducted a comparative analysis between their fractal resonator and a conventional unipolar resonator. The results indicated that the fractal resonator outperforms the conventional resonator in terms of both accuracy and sensitivity [21], [22], [23]. Utilizing this innovative cross-fractal sensor shows promise in revealing how fine-tuning the parameters of a 3D printer, specifically the 'infill percentage,' can influence permittivity (εr) and loss tangent (tan (δ)) by varying the infill percentage. Through the resonance frequency (fr) technique, it demonstrates a distinct sensitivity of 0.1822 GHz/RIU.

The effectiveness of this antenna was verified by simulating it with the CST program to be implemented in a private company ALMITECH. Next, we will characterize this antenna resonator by using the network analyzer to compare the experimental results with the simulation results. Finally, this resonator is used as a sensor to recognition of 3D printing properties in Polylactic Acid (PLA), of the difference of different dimensions of the same polyhedron and the size of the three polyhedrons (cube, cylinder and sphere). The proposed fractal antenna design has many potential applications, including surveillance systems and robotics. For example, resonators can be used in surveillance systems to detect human movements in robots and to track humanoid robots in industrial environments. In addition, the resonator can be used in industrial environments to monitor product quality and detect any other abnormalities. Fractal geometry has proven to be very useful in proposing small resonators [15], [16], [17], thanks to the advantages of fractal shapes. In this modest work, we have been able to create a fractal resonator with the properties of a sensor. This antenna allowed us to control and recognition of 3D printing properties of the difference in the sizes of objects (cube, cylinder and sphere).

The importance of this research lies in designing and developing a sensor capable of working with high characteristics that allow it to be connected with robots to augment their capacity to know the objects. This device can be used as an antenna and a sensor simultaneously, so this idea is new and has not been spoken before. The value of this sensor, its characteristics (sensitivity, selectivity, and linearity) were compared with recent works [19], [20], [21], [22], and it has proven effective in recognizing the objects. This is considered a contribution to the development of the field of smart robots and the AI applications. This sensor shows experimental miniaturization (with an electrical size of $\lambda_{0/}8$), a regular sensitivity of 0.004615 GHz/%, and good linearity in the frequency approach. This biosensor has successfully demonstrated its capacity to sense low concentrations of ethanol. These aqueous solutions, including familiar alcohols such as ethanol at low concentrations, permit the identification of halal and alcohol-free products in applications within the food sensor fields. This work focuses on the miniaturization and fabrication of a Novel Cross-Fractal Biosensor and Sensor designed to characterize 3D printing electromagnetic properties in Polylactic Acid (PLA). The uniqueness and innovation of this research lie in its distinctive capability to discern properties of both solid and liquid materials. This capability endows the biosensor and sensor with versatile functionalities, marking a significant advancement in the field. Most previous research has primarily addressed single-function sensing. This study stands out as the first to explore a multi-function sensor, representing a significant step for-

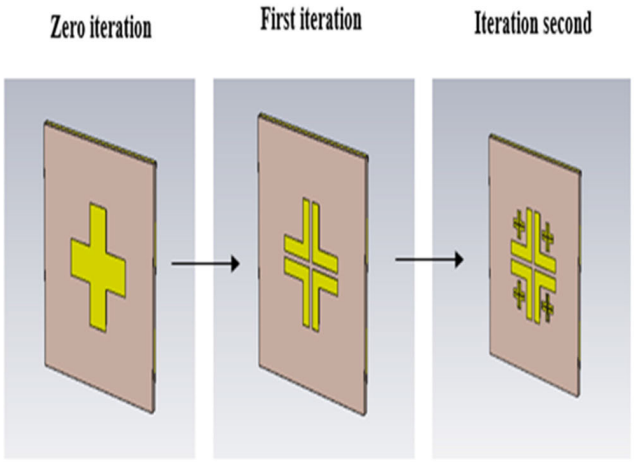

FIGURE 1. Consecutive repetitions of the novel cross fractal patch antenna.

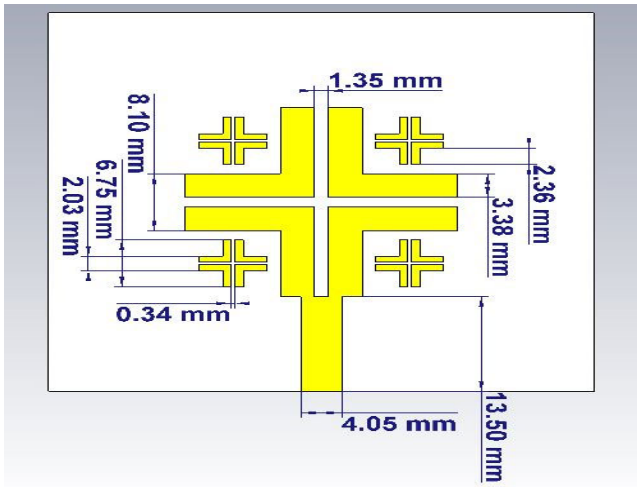

FIGURE 2. Schematic design of the novel cross fractal patch.

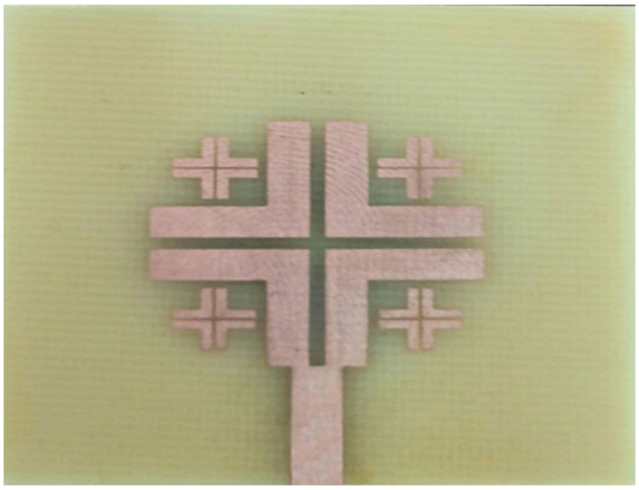

FIGURE 3. Photography of the new cross fractal resonator fabricated.

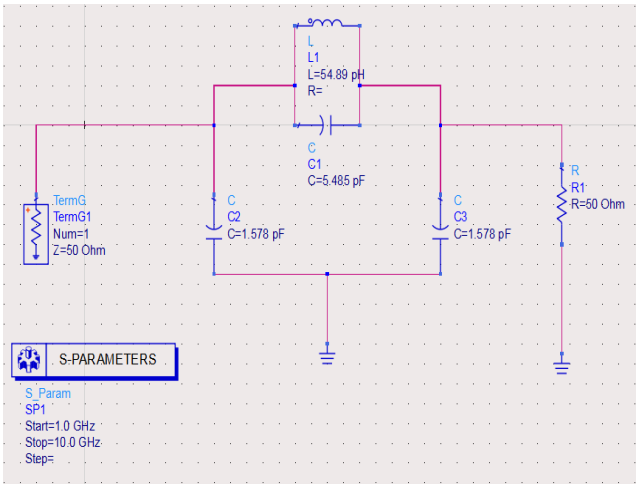

FIGURE 4. Equivalent circuit model of the novel sensor by ADS.

ward in the field of artificial intelligence, which relies on an approach closely resembling human functions.

II. DESIGN AND FABRICATION OF THE NEW CROSS-FRACTAL SENSOR

The cross-fractal geometry can be provided using an iterative that exhibits the characteristics of self-similar geometry [14]. In this optimization, the starting point is the structure shown in Fig. 1, the shape of which has been modified. The innovative cross fractal resonator is manufactured at the private SNC ALMITECH printed circuits center. This specific model was selected based on simulation results, demonstrating its ability to detect various objects. The resonators were manufactured on a dielectric substrate called FR4, with a thickness of 1.56 mm. The FR4 substrate has a relative permittivity of 4.3 and a loss tangent of 0.02. A metal pattern of 0.035 mm-thick copper was utilized, with a conductivity of $\sigma = 5.96 \times 107$ S/m. The dimensions of the cross-fractal patch can be observed in Fig. 2. The novel cross fractal sensor fabricated see the Fig. 3. The simulation software ADS based on the equivalent circuit of the novel sensor is shown in Figure 4.

III. 3D PRINTING OBJECTS IN POLYLACTIC ACID (PLA)

The 3D objects are fabricated in the mechanical construction laboratory of university using SolidWorks software, a 3D printer (see Fig. 5), and Polylactic Acid (PLA). PLA is one of the most usually materials used in 3D printing, being a recyclable polymer industrial from renewable resources. It possesses dielectric properties with a relative permittivity (εr) of 2.541 and a loss tangent (tan δ) of 0.0071, particularly when used with a 100% infill. The three shapes are realized (cube, cylinder, sphere see Fig. 6), with different dimensions. The following TABLE 1 presents the dimensions of the objects produced, in order to use them as samples to verify the effectiveness of the sensor for recognizing various volumes shapes.

IV. ANALYSIS OF THE NOVEL CROSS FRACTAL ANTENNA

The object of the study is not the properties of the antenna but its use as a sensor for objects detection, and this does not preclude presenting some results about the properties observed for the new cross antenna at The simulation by CST resonance frequency $f_r = 8.565$ GHz. The radiation pattern is an illustration of the antenna's radiation characteristics as

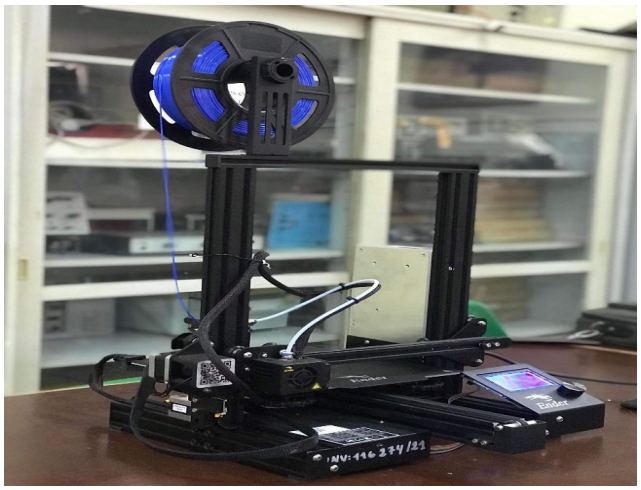

FIGURE 5. 3D printer used to fabricate the objects.

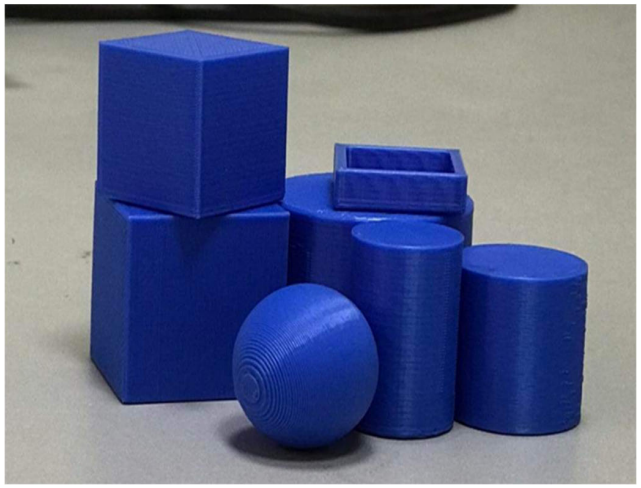

FIGURE 6. Photography of fabricated with 3D printer various forms of objects.

TABLE 1. The dimensions of the objects (cube, cylinder, sphere).

Form	Diameter/ side	Height
Cube 1	25mm	-
Cube 2	30mm	-
Cylinder 1	25mm	25mm
Cylinder 2	15mm	30mm
Sphere	25mm	-

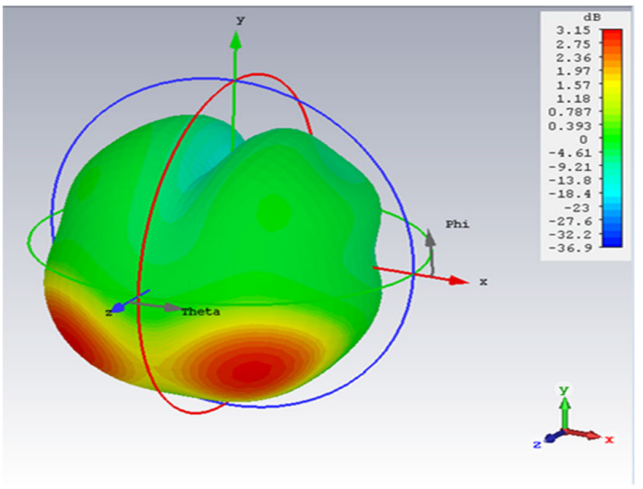

FIGURE 7. Three-dimensional radiation pattern of gain illustrated for the novel cross fractal antenna operating at 8.565 GHz.

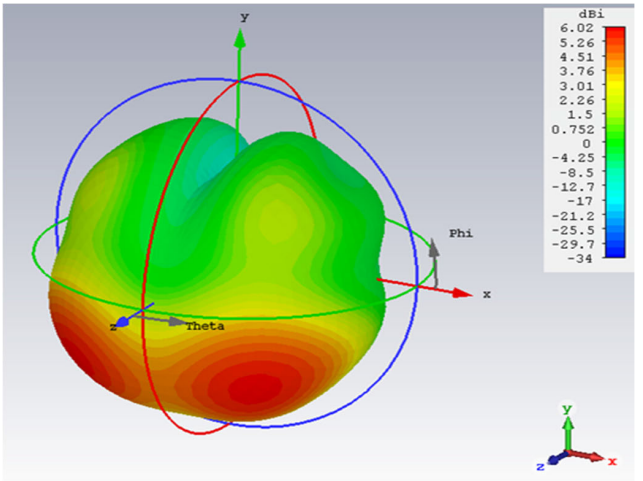

FIGURE 8. Three-dimensional radiation pattern of directivity illustrated for the novel cross fractal antenna operating at 8.565 GHz.

a function of spatial coordinates (Φ, θ). It is resolved in the far-field region, where the spatial distribution of radiated energy is independent of distance. Let's delve deeper into this characteristic. In Figs. 7 and 8, we present the 3D radiation pattern of gain and direction for the new fractal cross antenna operating at 8.565 GHz, along with specific patterns in the E-plane and H-plane. Evidently, the antenna predominantly radiates in the Z direction, exhibiting a highly favorable radiation pattern. Furthermore, it's noteworthy to examine the antenna's performance in the E-plane (i.e., Y-Z plane) at $\Phi = 90°$, as depicted in Fig. 9, and the H-plane (i.e., Y-Z plane) at $\theta = 90°$, as depicted in Fig. 10. It's worth emphasizing that the antenna emits precisely in the Z direction, with an extremely narrow -3 dB beam. The primary lobe along the Z direction spans an angular width of 65.3°. The study proves that this antenna is of high quality in terms of value directivity 6.02 dBi and gain 3.15 dB. To pinpoint the region of maximum sensitivity in the sensor, the current distribution is depicted for the new cross antenna at 8.565 GHz (see Fig. 11).

The network analyzer is used for the resonator characterization (see Fig. 12), but first we had to use an electronic calibration to eliminate measurement errors (S11=0) (see Fig. 13). After the calibration of the network analyzer, the characterization of the resonator is made (see Fig. 13). To ensure the convergence of the simulation results with the measurement outcomes, we performed an additional simulation based on the equivalent circuit. This conclusively demonstrated the consistency of results obtained through two distinct simulation methods: one utilizing the finite element method (FEM) with CST simulation software, and the other

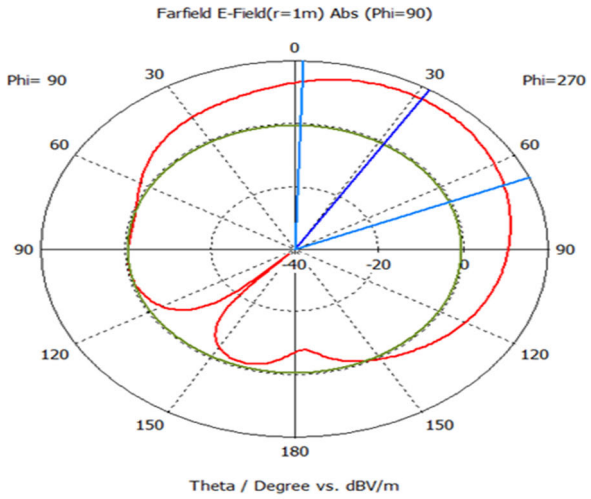

FIGURE 9. E-plane ($\Phi = 90°$) cross-sections illustrated for the new cross antenna at 8.565 GHz.

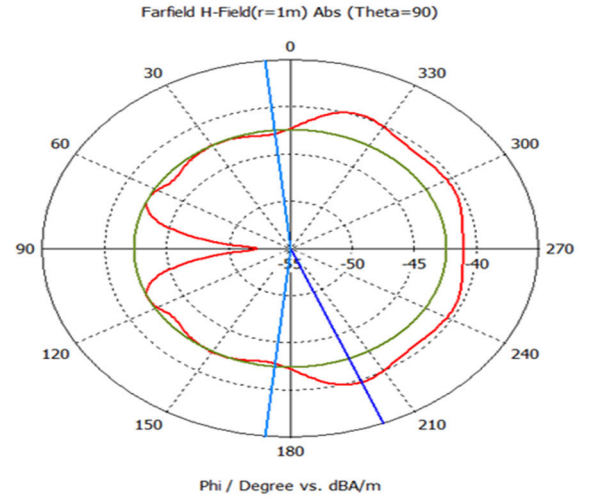

FIGURE 10. H-plane ($\theta = 90°$) cross-sections illustrated for the new cross antenna at 8.565 GHz.

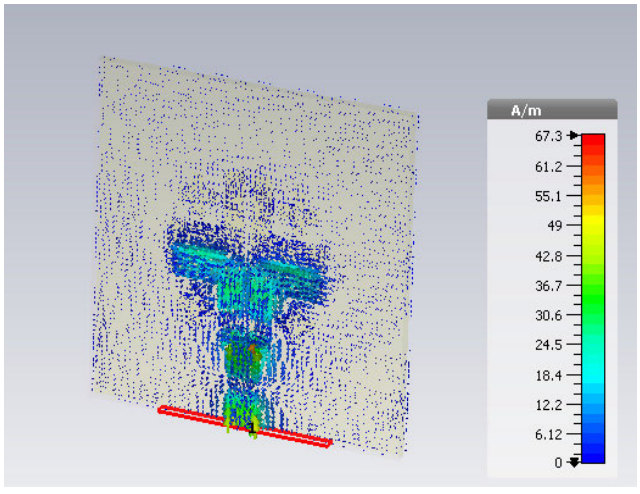

FIGURE 11. Current distribution illustrated for the new cross antenna at 8.565 GHz.

relying on the equivalent circuit with ADS simulation software.

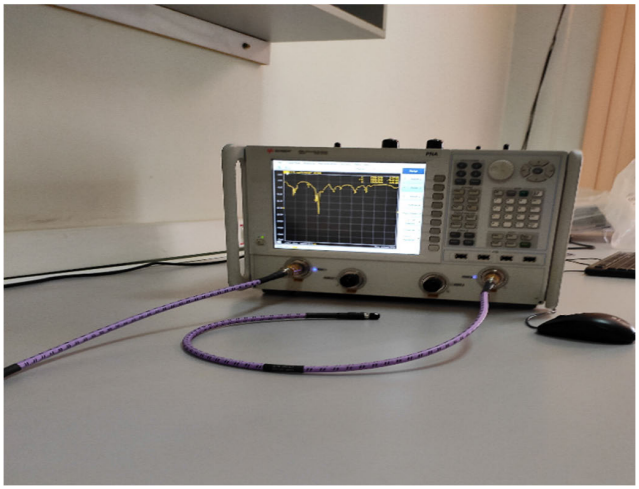

FIGURE 12. The network analyzer used.

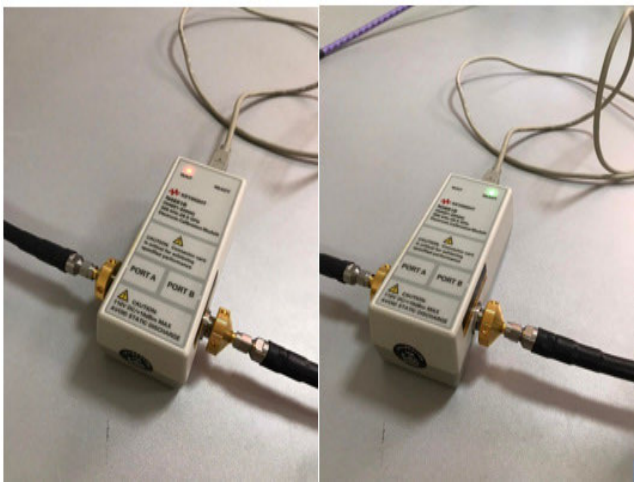

FIGURE 13. Network analyzer before and after calibration.

The results obtained from the network analyzer are illustrated in Figure 14 to enhance confidence in the convergence of simulation and measurement outcomes. Figures 15 and 16 depict the S11 curve, showcasing the simulated frequency response by CST and ADS, alongside the measured curve of the new cross-fractal resonator as provided by the network analyzer. A comparison of the two curves reveals close alignment between practical and simulated results. The resonance frequency obtained through CST simulation is $fr = 8.565$ GHz, while the resonance frequency from ADS simulation is $fr = 8.565$ GHz. The practical resonance frequency is also measured at $fr = 8.56$ GHz.

V. THE CROSS-FRACTAL-SHAPED SENSOR FOR RECOGNIZING 3D PRINTING PROPERTIES IN POLYLACTIC ACID (PLA).

In this work, the elementary characteristics of 3D printing in electromagnetism are briefly summarized. This is the primary difficult that always arises when using novel materials to make radiofrequencies devices [20]. This involves characterizing their electromagnetic properties in relations of dielectric constant (permittivity (ε_r)) and loss tangent ($\tan\delta$).

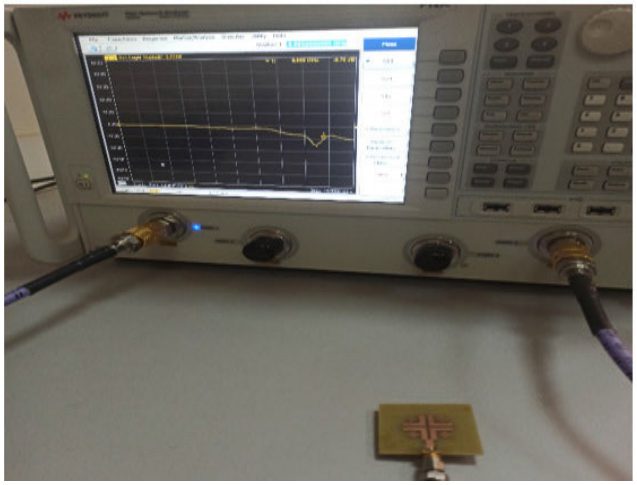

FIGURE 14. Analysis of the cross fractal resonator by network analyzer.

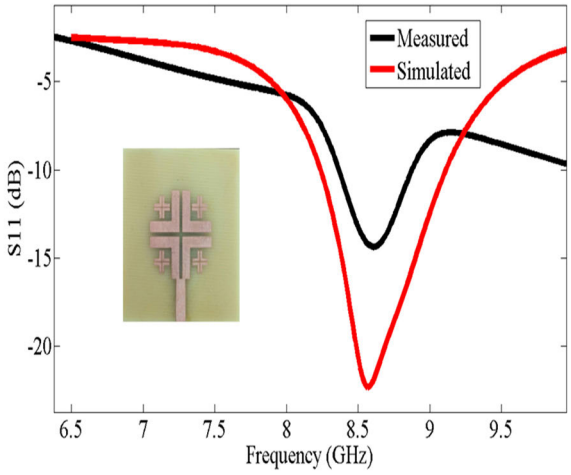

FIGURE 15. Simulated by CST and measured results of reflection response cross fractal resonator.

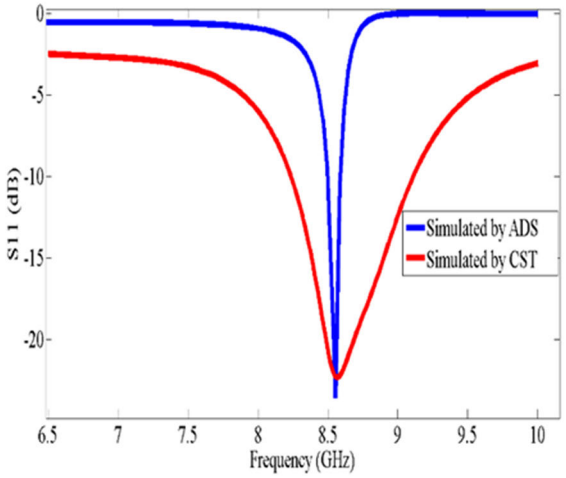

FIGURE 16. Simulated by ADS and Simulated by CST results of reflection response cross fractal resonator.

One approach to solve this problematic is to use this novel cross-shaped sensor for sensing characteristics of Polylactic acid (PLA) 3D printing (see Fig. 17). By employing this innovative cross-fractal sensor, there is potential to demonstrate

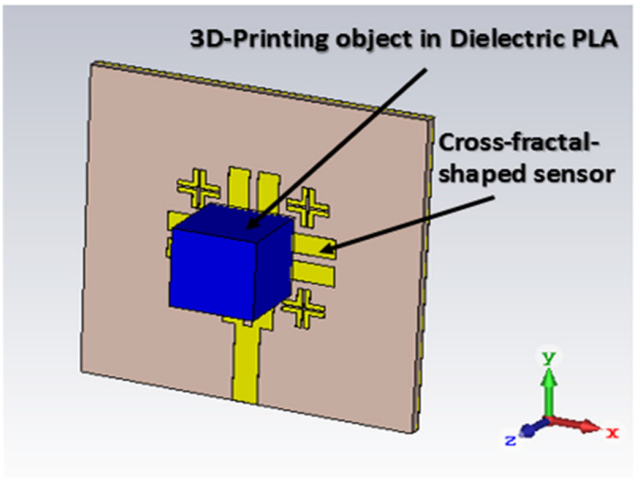

FIGURE 17. 3D-view of the cross-fractal-shaped sensor for recognizing 3D printing properties in Polylactic Acid (PLA).

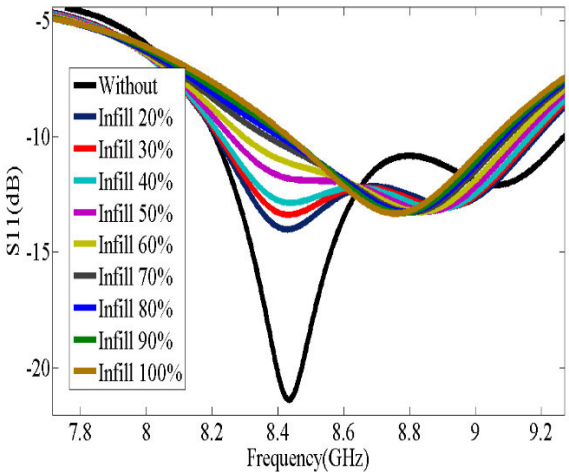

FIGURE 18. 3D-view of the cross-fractal-shaped sensor for recognizing 3D printing properties in Polylactic Acid (PLA).

how adjusting the 3D printer factors, specifically the 'infill percentage' of a 3D print, can result in variations in permittivity and loss tangent. This can be achieved through the utilization of the resonance frequency technique (see Fig. 18). When the 3D printer is configured to a specific filling ratio, it results in a change in electromagnetic properties for Polylactic acid printing, as the permittivity of the air affects the material's characteristics (see TABLE 2). As changes in permittivity are associated with variations in frequency, this sensor was specifically designed to detect the printing percentage with PLA. In the future, it can be extended to assess the printing quality with other materials

The linear curve fit of the dielectric PLA parameter ε_r by frequency approach (Fig.19), the line curve fit is found as follows,

$$\varepsilon r = -5.489 f_r + 50.57 \tag{1}$$

where the sensitivity S of this sensor is known by,

$$\mathbf{S}\,(\%) = \frac{\mathbf{\Delta fr}}{\mathbf{\Delta \varepsilon r}} \times 100\% \tag{2}$$

TABLE 2. Polylactic acid (PLA permittivity and loss-tangent with varying the infill percentage, the reflexion response (s_{11}), and the resonance frequency.

Infill %	Fr (GHz)	S11 (dB)	εr	tanδ
Without	9.064	-12.1	1	0
20%	8.926	-13	1.503	0.0031
30%	8.914	-13.08	1.578	0.0034
40%	8.896	-13.13	1.646	0.0035
50%	8.866	-13.23	1.8	0.0043
60%	8.833	-13.27	1.942	0.0048
70%	8.815	-13.27	2.13	0.0051
80%	8.8	-13.34	2.25	0.0054
90%	8.785	-13.31	2.371	0.0062
100%	8.755	-13.34	2.541	0.0071

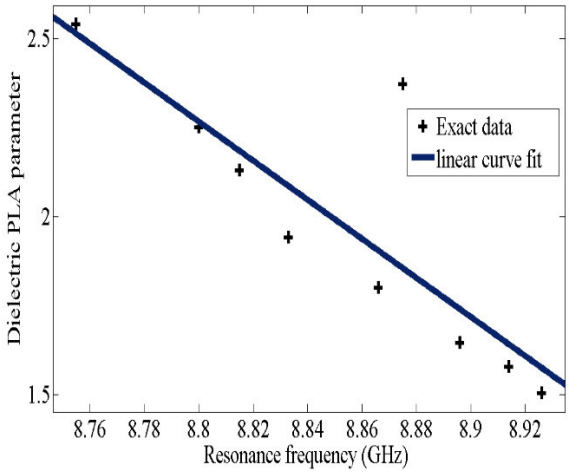

FIGURE 19. Linear curve fit of the dielectric PLA parameter ε_r vs. frequency (GHz).

Sensitivity is determined by the slope of the resonant frequency Δfr change in relation to the change in relative permittivity $\Delta \varepsilon r$. Where is found: S = 0.1822 GHz/RIU

The linear curve fit of the loss-tangent tan (δ) by frequency approach (Fig.20), the line curve fit is found as follows,

$$t\text{an}\delta = -0.01975 f_r + 0.1796 \tag{3}$$

where the sensitivity S of this sensor is given by,

$$\text{S}\,(\%) = \frac{\Delta fr}{\Delta tan\delta} \times 100\% \tag{4}$$

Sensitivity is determined by the slope of the resonant frequency Δfr change in relation to the change in the loss-tangent $\Delta \tan(\delta)$. Where is found: S = 50.633 GHz/RIU

Where RIU is the permittivity (εr) and the loss-tangent (tan (δ)) unit.

Figs. 19 and 20 illustrate a direct correlation between Dielectric PLA parameter and loss-tangent with varying the infill percentage and the resonance frequency. This relationship highlights the sensitivity of the sensor. At this moment, it's concluded that the sensor's antenna is working optimally in the characterization of the 3D printing electromagnetic properties in Polylactic Acid (PLA) in terms of permittivity (ε_r) and loss-tangent (tan (δ)).

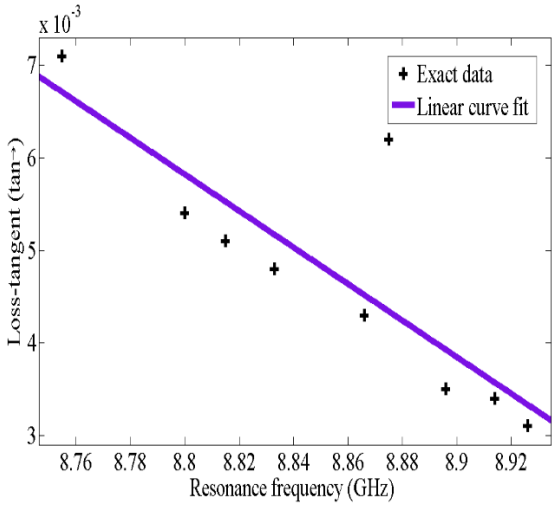

FIGURE 20. Linear curve fit of the loss-tangent tan (δ) vs. frequency (GHz).

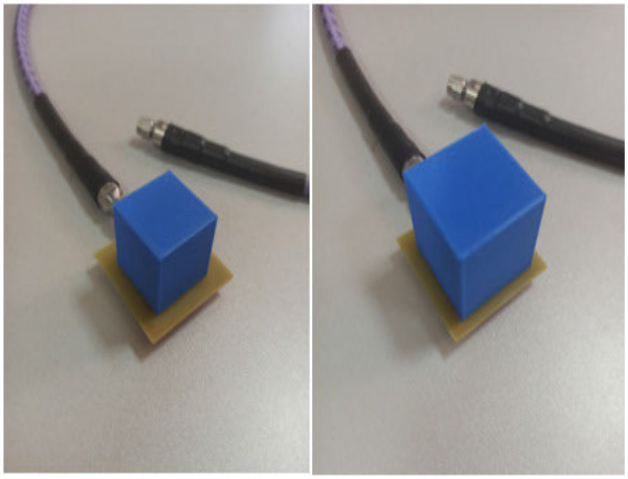

FIGURE 21. The control of cubes with side of 2.5 cm and 3.0 cm by network analyzer.

VI. DETECTION OF OBJECTS 3D PRINTING IN POLYLACTIC ACID (PLA) USING CROSS FRACTAL SENSOR

The cross fractal resonator was used as a sensor to detect the shape change of objects. For the control, we used two cubes 25mm and 30mm (see Fig. 21), the cubes are in the figure.19

According to the results presented in Fig.22 and TABLE 3, we notice a change of S11 according to the size of the cubes, when the size of the cubes increases, then the parameter S11 decreases. So, the parameter S11 decreases according to the contact surface of the object with the patch.

The results obtained are presented in the curves Fig. 23. According to the results presented in Fig.24 and TABLE 4, we notice a change of S11 according to the size of the

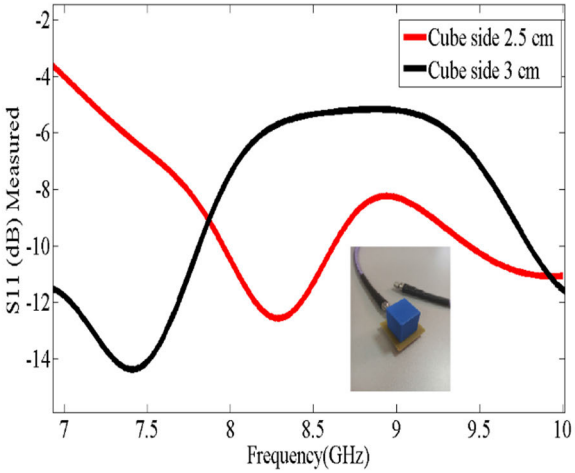

FIGURE 22. The measured reflection response of the cubes with changed dimensions.

TABLE 3. The resonance frequency variation and s11 as a function of the dimensions of the cubes.

Cubes Dimension	Fr(GHz)	S11 dB
Side 2.5 cm	8.38	-13.07
Side 3 cm	7.322	-15.18

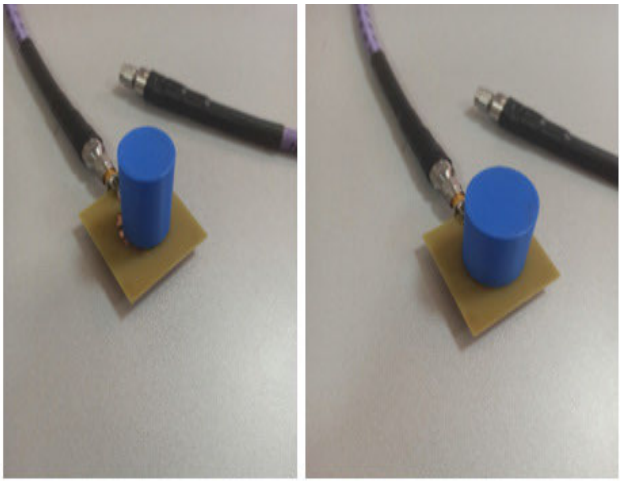

FIGURE 23. The control of cubes with side of 2.5 cm and 3.0 cm by network analyzer.

cylinders, when the size of the cylinders increases, and the parameter S11 decreases. So, the parameter S11 decreases according to the contact surface of the object with the patch. According to the results presented in TABLE 5 and Fig. 22-24, parameter S11 increases when we change the object's dimensions. So, parameter S11 decreases each time the contact surface of the object with the patch increases.

According to the applied results for comparing shapes of the same type, the sensor proved effective in identifying the difference through a change in the resonance frequency and reflection coefficient (S_{11}). After that, we compared different shapes to verify its ability to recognize objects of different volumes, and this was confirmed through the applied results. This confirms the effectiveness of the sensor. According to

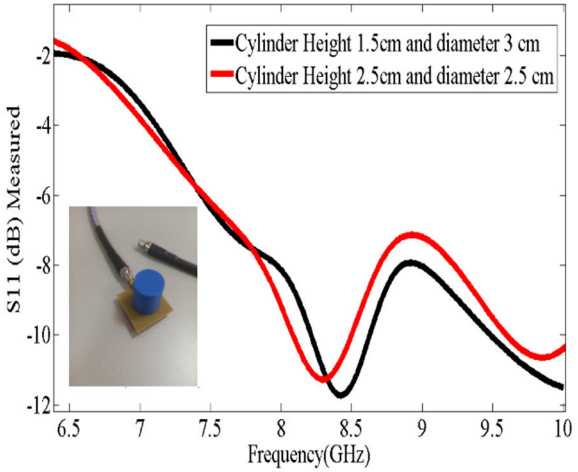

FIGURE 24. The measured reflection response of the cylinders with changed dimensions.

TABLE 4. The resonance frequency variation and S11 as a function of the dimensions of the cubes.

Cylinders Dimensions	Fr (GHz)	S_{11} (dB)
Height 2.5 cm/ Diameter 2.5 cm	8.268	-12.02
Height 1.5 cm / Diameter 3 cm	8.38	-12.10

TABLE 5. The reflexion response (s_{11}) and resonance frequency vs. volumes of objects.

Shapes Anthropomorphic	Fr (GHz)	S11 (dB)	Volume (cm^3)
Cube with Side 2.5 cm	8.268	-13.33	15.625
Cylinder with Height 2.5 cm and Diameter 2.5 cm	8.357	-12.02	12.272
Sphere with Diameter 2.5 cm	8.492	-11.03	8.181

the curves from Figs. 21 to 27, our resonator works well, it detects size variation of objects (same shape) and volume variation of three different objects (form detection), from which our resonator is selective and from the result of fitting curves the resonator achieves linearity and gives us resonator sensitivity, then we can treat this cross fractal resonator as a sensor. The analysis demonstrated that this new cross fractal resonator-based realization sensor has the high sensitivity and high linearity of this new device with two approaches:

The frequency technique has a typical sensitivity of 0.0302 GHz/cm^3 and the parameter technique S11 has a typical sensitivity of 0.3065 dB/cm^3.

According to the applied results for comparing shapes of the same type, the sensor proved effective in identifying the difference through a change in the resonance frequency and reflection coefficient (S11). After that, we compared different shapes to verify its ability to recognize objects of different volumes, and this was confirmed through the applied results. This confirms the effectiveness of the sensor.

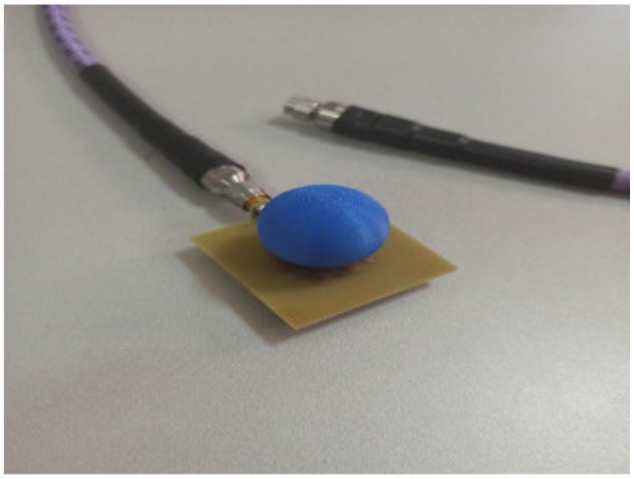

FIGURE 25. The control of sphere with radius of 25mm by network analyzer.

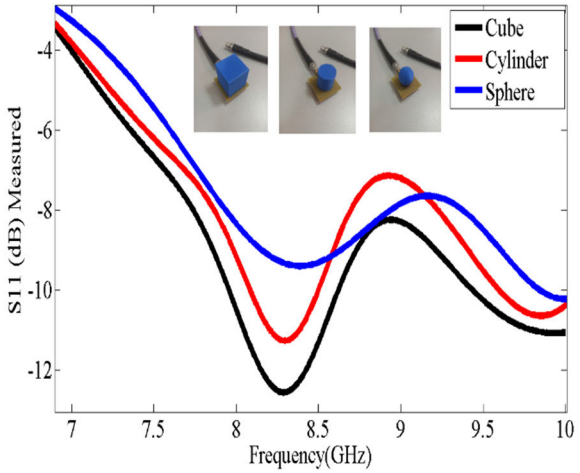

FIGURE 26. The measured reflection response of volume of three anthropomorphic shapes (cube, cylinder; and sphere).

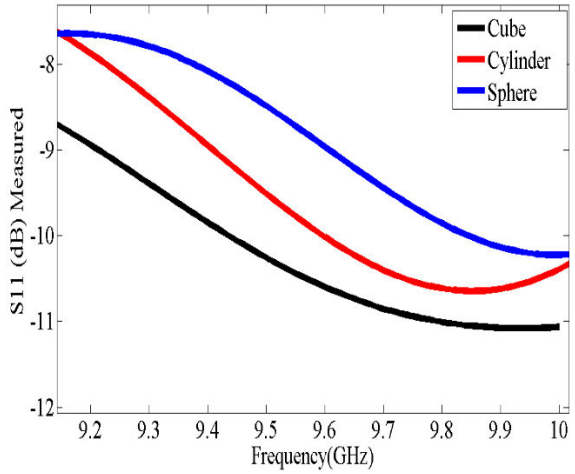

FIGURE 27. The zoomed results detection of three objects.

The curve fit frequency technique (Fig.28), the line curve fit is found as follows,

$$fr = -0.0302\text{V} + 8.735 \tag{5}$$

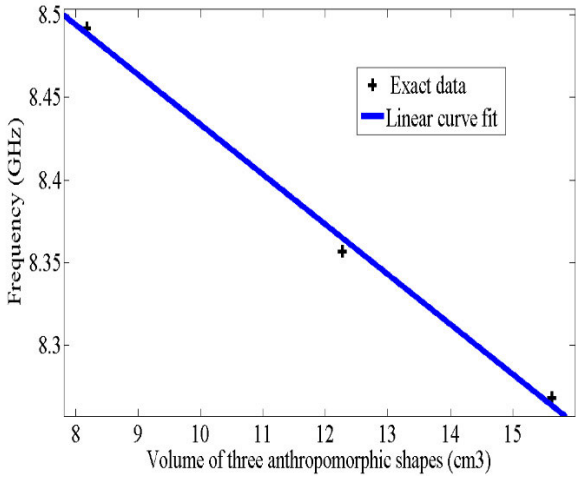

FIGURE 28. The linear curve fit of volume of three anthropomorphic shapes vs. frequency (GHz).

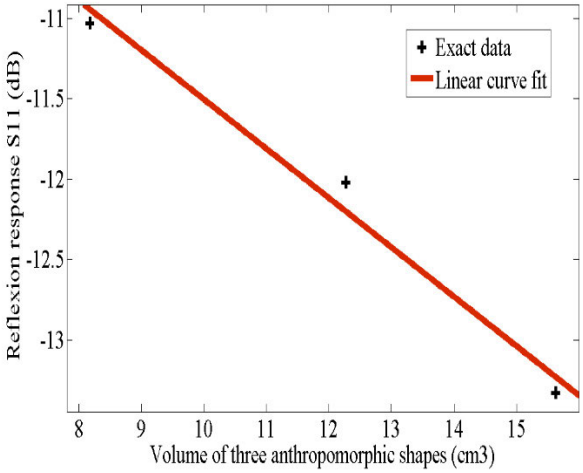

FIGURE 29. The linear curve fit of volume of three anthropomorphic shapes vs. reflection coefficient (S_{11}).

The curve fit reflection coefficient (S11) approach (Fig.29), the line curve fit is found as follows,

$$S11 = -0.3065\text{V} - 8.44 \tag{6}$$

where the sensitivity S of this instrument are given by,

$$\text{S}\,(\%) = \frac{\Delta fr}{\Delta V} \times 100\% \tag{7}$$

$$\text{S}\,(\%) = \frac{\Delta \text{S11}}{\Delta V} \times 100\% \tag{8}$$

Sensitivity is determined by the slope of the resonant frequency Δfr (or the reflection coefficient ΔS_{11}) change in relation to the change in object volume ΔV. Where the sensitivities are found:

S= 0.0302 GHz/cm^3

S=-0.3065dB/cm^3

VII. BIOSENSOR CROSS FRACTAL FOR ETHANOL CONCENTRATION DETECTION

Fig. 10 illustrates the radiofrequency measurement system employing a vector network analyzer for the suggested proposal with varying concentrations of ethanol. In Fig. 30, the

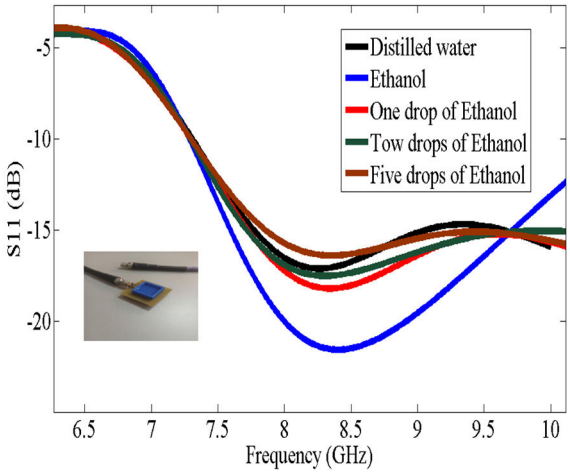

FIGURE 30. The measured reflection response of detection of alcohol using cross fractal biosensor.

TABLE 6. The reflexion response (S11) and resonance frequency vs. concentrations of water-ethanol.

Liquid	Fr (GHz)	S11 (dB)
Distilled water	8.263	-21.56
Pure Ethanol	8.43	-17.12
Drop of ethanol in distilled water	8.35	-18.21
Two drops of ethanol in distilled water	8.34	-17.52
Five drops of ethanol in distilled water	8.33	-16.4

measured reflection scattering parameter S11 is presented for different concentrations of water-ethanol. It is noticeable that the resonance frequency shifts from 6.5 GHz to 10 GHz as the ethanol concentrations range from 1% to 5% in deionized water at 25°C (for detailed data, please refer to TABLE 6).

The series of measurements aimed to assess the biosensor's capability to detect low concentrations of ethanol in a liquid. TABLE 7 and Figure 31 demonstrate an increase in resonant frequency with each increment in ethanol concentration in the liquid. Conversely, the decrease is observed in the frequency shift to approximately 10 MHz when ethanol concentrations range from 1% to 5% in deionized water without sugar.

The linear curve fit frequency method (Fig.31), we have the line curve fit as follows,

$$fr = 0.004615\mathrm{C} + 8.328 \tag{9}$$

where the sensitivity S of this sensor is given by,

$$\mathrm{S}\,(\%) = \frac{\Delta fr}{\Delta C} \times 100\% \tag{10}$$

Sensitivity is determined by the slope of the resonant frequency Δfr change in relation to the change in ethanol concentration ΔC.We find: S = 0.004615 GHz/%

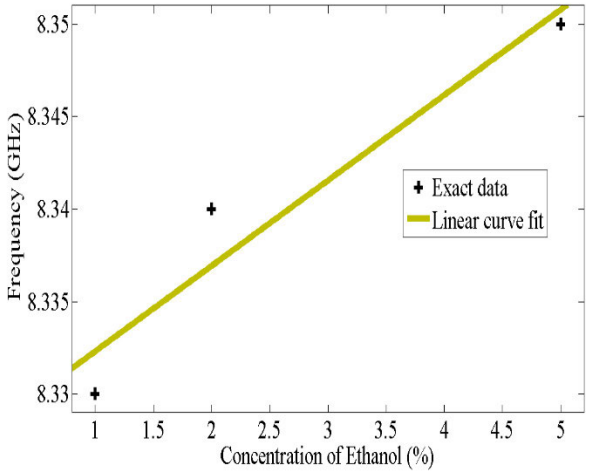

FIGURE 31. The measured reflection response of detection of alcohol using cross fractal biosensor.

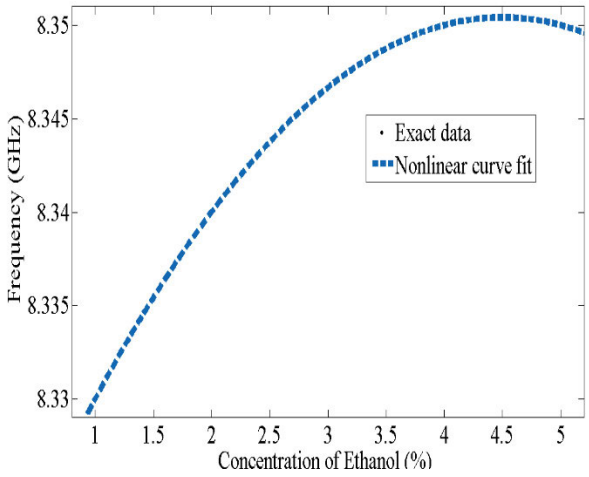

FIGURE 32. The measured reflection response of detection of alcohol using cross fractal biosensor.

The nonlinear curve fit frequency method (Fig.32), we have the function curve fit as follows,

$$fr = -0.001667C^2 + 0.015C + 8.317 \tag{11}$$

Figures 31 and 32 depict a direct correlation between the concentration of ethanol (%) and the resonance frequency. This relationship highlights the sensitivity of the biosensor. At this juncture, the biosensor's antenna is functioning optimally in the identification of Halal and alcohol-free products within the fields of food and biomedical sensor applications.

The present work includes a comprehensive comparison between the types of resonators used for sensor in the present study and the resonators used in this study. The main objective was to evaluate and highlight the performance and advantages of this new sensor by comparing it with similar devices (as shown in TABLE 7). This comparison demonstrates the effectiveness and importance of the sensor compared to existing alternatives, thereby confirming the results of this study. By comparing dimensions, this model has shown the potential for miniaturization and exhibits favorable characteristics. The comparison of the two methods has demonstrated remarkable

TABLE 7. Comparison between our resonator form measurement and some existing works.

Important Parameter	2023 [21]	2023 [22]	2023 [23]	This Work
Material	Rogers	FR4	FR4	**FR4**
Resonator Topology	Slotted cylindrical resonator	Hybrid plus fractal	SRR with Minkowski fractal	**Fractal resonator**
S_{11} dB variation by liquid	11.68	**13.3**	−36.97	**-13.63**
Required test liquid Volume (mm3)	~900	720	Not mention	**300**
Operation frequency Range (empty to water)	2.39–2.51 GHz	2-2.5 GHz	3.8-4 GHz	**8.3-8.6 GHz**
Sensitivity (DI Water for S	Not mention	Frequency method : 0.132 S11 parameter method : 0.1862	Not mention	**Frequency method : 0.004615 S11 parameter method : 0.001667**
Gain [dB]	4.02	2	2.28	**3.15**
Design size [mm^2]	10 x10	38 x38	12 ×18	**10 x 10**
Fabrication Process	Very easy (Standard PCB)	Very easy (Standard PCB)	Very easy (Standard PCB)	**Very easy (Standard PCB)**

convergence in terms of sensitivity and linearity. It confirms the proposed sensor's ability to rely on both methods in a robust and reliable manner.

VIII. CONCLUSION

In conclusion, the detection of anthropomorphic forms is an important characteristic of many recent AI technologies, and the advancement of novel tools capable of identifying these forms is fundamental. The fractal sensor has shown great competence in this area and the cross-fractal sensor design suggested in this work represents an important phase forward in the development of these technologies. With promote research and development, the fractal sensor could become a key technology in detecting volumes shapes. We simulated a new fractal pattern proposed in this work as a cross, which is less complex and gives good results. This proposed fractal model is realized and characterized, the results of the parameter S11 given by the measurement are consistent with the simulation results. The sensor works well and detects the object change well, the characteristics of this sensor are sensitive, linear, and selective and fast. The study of sensor shows miniaturization (with an electrical size of $\lambda_0/8$), high sensitivity, and excellent linearity in the experimental frequency method, boasting an average sensitivity of 0.004615 GHz/C%. The proposed biosensor has verified its capability to sense low concentrations of Ethanol. These aqueous solutions, including known alcohols like ethanol at low concentrations, empower the identification of halal and alcohol-free products in applications within the agro-food sensor fields. Paying this cross-fractal sensor holds potential for unveiling the impact of fine-tuning 3D printer parameters, particularly the 'infill percentage,' on permittivity (εr) and loss tangent ($\tan(\delta)$), as they vary with the infill percentage. Utilizing the resonance frequency method, it showcases an important sensitivity of 0.1822 GHz/RIU. The novelty and originality of this research lie in its capacity to identify both solid and liquid materials, providing it with multifunctional capabilities.

ACKNOWLEDGMENT

The authors would like to acknowledge the Deanship of Graduate Studies and Scientific Research, Taif University for funding this work.

REFERENCES

[1] B. Mandelbrot, *The Fractal Geometry Nature*. New York, NY, USA: W.H. Freeman and Company, 1975.
[2] G. Cataldi, A. Abedi, G. Magnifico, S. Notarnicola, N. D. Pozza, V. Giovannetti, and S. Montangero, "Hilbert curve vs Hilbert space: Exploiting fractal 2D covering to increase tensor network efficiency," *Quantum*, vol. 5, p. 556, Sep. 2021.
[3] S. Mythili, K. Akshaya, and B. Charanya, "Design and analysis of Koch fractal antenna for WLAN applications," *ICTACT J. Microelectron.*, vol. 6, no. 2, pp. 923–927, 2020.
[4] D. Kaushal and T. Shanmuganantham, "Parametric enhancement of a novel microstrip patch antenna using circular SRR loaded fractal geometry," *Alexandria Eng. J.*, vol. 57, no. 4, pp. 2551–2557, Dec. 2018.
[5] S. M. K. Azam, M. Othman, H. A. Illias, T. Abdul Latef, M. Tariqul Islam, and M. Fadzil Ain, "Ultra-high frequency printable antennas for partial discharge diagnostics in high voltage equipment," *Alexandria Eng. J.*, vol. 64, pp. 709–729, Feb. 2023.
[6] O. Benkhadda, M. Saih, S. Ahmad, A. J. A. Al-Gburi, Z. Zakaria, K. Chaji, and A. Reha, "A miniaturized tri-wideband Sierpinski hexagonal-shaped fractal antenna for wireless communication applications," *Fractal Fractional*, vol. 7, no. 2, p. 115, Jan. 2023.
[7] M. Marzouk, Y. Rhazi, I. H. Nejdi, F.-E. Zerrad, M. Saih, S. Ahmad, A. Ghaffar, and M. Hussein, "Ultra-wideband compact fractal antenna for WiMAX, WLAN, C and X band applications," *Sensors*, vol. 23, no. 9, p. 4254, Apr. 2023.
[8] G. B. Kalkhambkar, R. Khanai, and P. Chindhi, "A novel diagonally symmetric fractal antenna with wideband characteristics for Internet of Things applications," *Prog. Electromagn. Res. C*, vol. 131, pp. 145–158, 2023.
[9] I. H. Nejdi, S. Bri, M. Marzouk, S. Ahmad, Y. Rhazi, M. A. Lafkih, Y. A. Sheikh, A. Ghaffar, and M. Hussein, "UWB circular fractal antenna with high gain for telecommunication applications," *Sensors*, vol. 23, no. 8, p. 4172, Apr. 2023.
[10] C. Elavarasi and T. Shanmuganantham, "Multiband SRR loaded Koch star fractal antenna," *Alexandria Eng. J.*, vol. 57, no. 3, pp. 1549–1555, Sep. 2018.
[11] A. Karmakar, "Fractal antennas and arrays: A review and recent developments," *Int. J. Microw. Wireless Technol.*, vol. 13, no. 2, pp. 173–197, Mar. 2021.
[12] N. Kaur, J. Singh, and M. Kumar, "Hexagonal ring shaped dual band antenna using staircase fractal geometry for wireless applications," *Wireless Pers. Commun.*, vol. 113, no. 4, pp. 2067–2078, Aug. 2020.
[13] K. Pedram, J. Nourinia, C. Ghobadi, N. Pouyanfar, and M. Karamirad, "Compact and miniaturized metamaterial-based microstrip fractal antenna with reconfigurable qualification," *AEU Int. J. Electron. Commun.*, vol. 114, Feb. 2020, Art. no. 152959.
[14] Z. Mezache, "Analysis of multiband graphene-based terahertz square-ring fractal antenna," *Ukrainian J. Phys. Opt.*, vol. 21, no. 2, pp. 93–102, 2020.
[15] M. N. Moghadasi, R. A. Sadeghzadeh, M. Toolabi, P. Jahangiri, and F. B. Zarrabi, "Fractal cross aperture nano-antenna with graphene coat for bio-sensing application," *Microelectronic Eng.*, vol. 162, pp. 1–5, Aug. 2016.

[16] N. Alrayes and M. I. Hussein, "Metamaterial-based sensor design using split ring resonator and Hilbert fractal for biomedical application," *Sens. Bio-Sens. Res.*, vol. 31, Feb. 2021, Art. no. 100395.
[17] P. Deka and A. De, "Design of fractal antenna for multiband operation in communication and healthcare," in *Proc. 2nd Global Conf. Advancement Technol. (GCAT)*, Oct. 2021, pp. 1–4.
[18] H. T. Sediq, J. Nourinia, C. Ghobadi, and B. Mohammadi, "A novel shaped ultrawideband fractal antenna for medical purposes," *Biomed. Signal Process. Control*, vol. 80, Feb. 2023, Art. no. 104363.
[19] A. R. Chishti, A. Aziz, M. A. Qureshi, M. N. Abbasi, D. Abbasi, S. S. Iqbal, A. Zerguine, A. M. Algarni, and R. Hussain, "Advances in antenna-based techniques for detection and monitoring of critical chronic diseases: A comprehensive review," *IEEE Access*, vol. 11, pp. 104463–104484, 2023.
[20] R. Colella, F. P. Chietera, and L. Catarinucci, "Analysis of FDM and DLP 3D-printing technologies to prototype electromagnetic devices for RFID applications," *Sensors*, vol. 21, no. 3, p. 897, Jan. 2021.
[21] M. H. B. Ucar and E. Uras, "A compact modified two-arm rectangular spiral implantable antenna design for ISM band biosensing applications," *Sensors*, vol. 23, no. 10, p. 4883, May 2023.
[22] Z. Mezache, A. Mansoul, and A. H. Merabet, "Accuracy and precision of sensing fructose concentration in water using new fractal antenna biosensor," *Appl. Phys. A, Solids Surf.*, vol. 129, no. 4, p. 267, Apr. 2023.
[23] V. Jagadeesan, D. Venkatachalam, V. M. Vinod, A. K. Loganathan, S. Muthusamy, M. Krishnamoorthy, K. K. Sadasivuni, and M. Geetha, "Design and development of a new metamaterial sensor-based Minkowski fractal antenna for medical imaging," *Appl. Phys. A, Solids Surf.*, vol. 129, no. 5, p. 391, May 2023.

MEZACHE ZINELABIDDINE was born in Chelghoum Laïd, Algeria, in 2016. He received the M.Sc. and Ph.D. degrees in electronics from the University of Constantine 1, Constantine, Algeria. He has been a Full Professor with the Institute of Optics and Fine Mechanics, University of Ferhat Abbas Setif 1, Setif, Algeria, since 2017.

ABDULLAH ALZAHRANI was a Research Associate of electronic smart sensors with the Department of Electrical Engineering, Cambridge Graphene Center (CGC), University of Cambridge, U.K. Before joining the university, he worked at different institutes, such as the College of Technology, Saudi Arabia, and Loughborough University, U.K. He also worked at start-up companies, such as Cerebrum Matter Ltd., U.K., that specialized in EEG and Alzheimer's. He is currently an Assistant Professor with Taif University. His research interest includes sensor fabrications.

ABDULLAH ALWABLI received the B.Sc. degree in electrical engineering from Umm-Al-Qura University, Saudi Arabia, in 2012, and the Ph.D. degree in electrical engineering from Florida Institute of Technology, USA, in 2021. Since 2021, he has been an Assistant Professor with the College of Communication and Electronics Engineering, Umm-Al-Qura University. His research interests include radio communication, cellular systems, wireless sensor networks, and radar systems.

AMAR JAFFAR received the B.S. degree in computer engineering from Umm Al Qura University, Makkah, Saudi Arabia, in 2006, the M.S. degree in electrical engineering from the University of New Haven, New Haven, USA, in 2012, and the Ph.D. degree in computer engineering from Florida Institute of Technology, USA, in 2019. From 2007 to 2010, he was a Lecturer with the Computer Engineering Department, Umm Al-Qura University. Since 2019, he has been an Assistant Professor with the College of Computing, Umm-Al-Qura University. His research interests include WSN deployment, AI applications, the Internet of Things, network security, and system-on-chip.

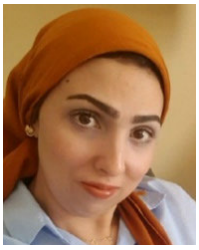

ENAS ALI received the Ph.D. degree, in 2021. She is currently an Adjunct Assistant Professor with the Research Impact and Outcome Center, Chitkara University Institute of Engineering and Technology, Rajpura, Punjab, India. Her research interest includes artificial intelligence applications.

MOHAMMED S. ALZAIDI received the B.Sc. degree in electrical engineering from Umm Al-Qura University, Makkah, Saudi Arabia, in 2007, and the M.Eng. and Ph.D. degrees in electrical engineering from the Stevens Institute of Technology, Hoboken, NJ, USA, in 2014 and 2019, respectively. He is currently an Associate Professor with the Department of Electrical Engineering, Faculty of Engineering, Taif University, Saudi Arabia. He is also the Vice Dean of the Deanship of Graduate Studies and Scientific Research for Scientific Research with Taif University. His research interests include molecular communications, wireless communications, signal processing, and digital techniques.